Sodium-hydrogen exchangers in *C. elegans*: Investigations towards their potential role in hypodermal H^+ excretion, Na^+ uptake and ammonia excretion as well as acid-base balance

[1]Aida Adlimoghaddam, [2]Michael J. O'Donnell, Alex Quijada-Rodriguez, and [1]Dirk Weihrauch*

Aida Adlimoghaddam: University of Manitoba, Winnipeg, MB, R3T2N2, Canada; Aida.Adlimoghaddam@umanitoba.ca.

[2]Michael J. O'Donnell: Department of Biology, McMaster University, Hamilton, ON, L8S 4K1, Canada ; odonnell@mcmaster.ca.

Alex Quijada-Rodriguez: University of Manitoba, Winnipeg, MB, R3T2N2, Canada; umquijaa@myumanitoba.ca.

*Dirk Weihrauch: Author for correspondence, University of Manitoba, Winnipeg, MB, R3T2N2, Canada, Phone: 204 4746310, Fax: 204 4747604, Dirk.Weihrauch@umanitoba.ca.

Keywords: Amiloride, EIPA, SIET, NHE, Hypodermis, Na^+ channel, C. elegans

Abstract

Cation/proton exchangers of the Cation proton antiporter 1 (CPA1) subfamily (NHEs, SLC 9) play an important role in many physiological processes, including cell volume regulation, acid-base homeostasis and ammonia excretion. The soil nematode *Caenorhabditis elegans* expresses nine paralogues (NHX-1 to -9). The current study was undertaken to investigate the role of the cation/proton exchanger in hypodermal Na^+ and H^+ fluxes as well in ammonia excretion processes. Measurements using the scanning ion-selective electrode technique (SIET) showed that the hypodermis promotes H^+ secretion as well as a Na^+ uptake. Interestingly, while both fluxes, as well as whole body ammonia excretion rates were partially inhibited by amiloride (100 µmol l^{-1}), no effect was observed on the H^+ efflux and ammonia excretion rates when animals were exposed to 100 µmol l^{-1} EIPA, suggesting rather the participation of apical Na^+ channels in the Na^+ uptake process, but probably not NHX transporters. In response to stress induced by starvation or exposure to 1 mmol l^{-1} NH_4Cl (HEA), pH = 5.5, pH = 8.0), body pH stayed fairly constant, with changes of mRNA expression levels detected in intestinal NHX-2 and hypodermal NHX-3. Excretory cell NHX-9 mRNA expression was altered by exposure to pH 5.5 or 8.0 but not by HEA. In conclusion, the study suggest that hypodermal apically localized EIPA-sensitive sodium/hydrogen exchangers do likely not play a role in ammonia excretion and Na^+ uptake in the hypodermis of *C. elegans*, while apical amiloride sensitive Na^+ channels seems to be involved not just in hypodermal Na^+ uptake, but indirectly also in NH_4^+ and H^+ excretion.

Introduction

Members of solute carrier family 9 (NHEs, cation/proton exchangers, SLC 9) belong to the Cation proton antiporter 1 (CPA1) subfamily and play an important role in diverse physiological processes by facilitating monovalent cation/proton exchange across cell membranes and membranes of intracellular organelles. Transporting Na^+ or K^+ in exchange for protons, NHEs are primarily involved in the regulation of cellular and organellar pH as well as in cell volume adjustment (Orlowski and Grinstein 2004; Zachos et al. 2005). Although sometimes driven by a V-ATPase, e.g. in the Malpighian tubules of mosquitoes (Wieczorek et al. 2009), cation/proton exchangers are commonly energized by the Na^+/K^+-ATPase, which generates w low intracellular Na^+ concentration that drive Na^+ in and H^+ out of the cytoplasm. In aquatic animals NHEs have been implicated to be involved in branchial osmoregulatory Na^+ uptake mechanisms observed e.g. in fish (Edwards et al. 1999; Hirata et al. 2003; Scott et al. 2005; Wilson et al. 2000) and crustaceans (Towle et al. 1997; Towle and Weihrauch 2001). In addition, NHEs have also been associated with transepithelial ammonia transport. The apical NHE-3 has been suggested to play a role in mammalian renal ammonia transport (Weiner and Hamm 2007; Nagami 1988), while earlier studies showed Na^+/NH_4^+ exchange activity in nephridial brush border vesicles prepared from the proximal tubule (Kinsella and Aronson 1981). Also, in the midgut epithelium of the tobacco hornworm *Manduca sexta,* an as yet uncharacterized amiloride- and 5-(N-Ethyl-N-isopropyl) amiloride (EIPA)-sensitive cation/H^+ antiporter has been implicated in transport of NH_4^+ from the alkaline gut lumen into the cytoplasm in exchange for protons (Weihrauch 2006; Blaesse et al. 2010). Although it has only been suggested that cation/H^+ exchangers may transport NH_4^+ ions directly, it is generally accepted that these transporters can facilitate the acidification of the apical unstirred boundary layer in ammonia

excreting epithelia and thereby generate an outwardly directed partial pressure gradient for NH_3. Accordingly, an NHE facilitated ammonia excretion mechanism was suggested for trans-epidermal ammonia excretion in the freshwater planarian *Schmidtea mediterranea* (Weihrauch et al. 2012), and also for branchial ammonia excretion in the pufferfish *Takifugu rubripes* (Nawata et al. 2010) and the amphibious mudskipper *Periophthalmodon schlosseri* (Randall et al. 1999). Moreover, Wright and Wood proposed a general model for ammonia excretion in freshwater fish, suggesting an apical "Na^+/NH_4^+ exchange complex", where several membrane transporters, including Rh-proteins, V-ATPase, NHE-2 and/or NHE-3 and Na^+ channels operate together as a metabolon to provide a mechanism for acid trapping of ammonia on the apical surface (Wright and Wood 2009).

Sodium/hydrogen exchangers have been most thoroughly studied in mammals, and NHE-1 is likely the best-understood transporter of the NHE family (Wakabayashi et al. 2000; Slepkov et al. 2005; Slepkov et al. 2007). For NHE-1, the N-terminal membrane domain is necessary and sufficient for ion translocation (Wakabayashi et al. 1992; Murtazina et al. 2001; Touret et al. 2001), while the C-terminus is important for regulatory functions. Numerous phosphorylation sites for various protein kinases and other sites responsible for interaction with accessory proteins are localized in the C-terminus (Orlowski and Grinstein 2004; Slepkov et al. 2007). Part of the ion conduction pathway is the fourth transmembrane domain (TM4) (Slepkov et al. 2005). This domain also contains the nine amino acid amiloride binding motif "$\mathbf{F_1 \cdot F_2 \cdot} X_3 \cdot X_4 \cdot X_5 \cdot \mathbf{L_6 \cdot P_7 \cdot P_8 \cdot I_9}$", that is conserved in members of the NHE family (Counillon et al. 1993; Counillon et al. 1997) (figure 1).

In the genetic model system *Caenorhabditis elegans* 9 putative NHE homologs have been cloned (called NHX-1 through -9) and investigated for their tissue and cellular localization in the

nematode (Nehrke and Melvin 2002). The authors reported that NHX-1 showed expression in a multicomponent pattern in hypodermal and muscle cells over the entire length of the worm. NHX-2, -6 and -7 were found in the intestine, with NHX-2 localized to the apical membrane and NHX-7 localized predominantly to the basolateral membrane. NHX-6 is also localized to the basolateral membrane, but only in the most anterior and most posterior regions of the intestine. NHX-4 was evidently expressed in all cell types. In polarized cells, NHX-4 was targeted to the basolateral membrane and was therefore compared to the ubiquitously expressed mammalian NHE-1. In contrast to the NHX isoforms mentioned above, NHX-3, -5, -8 and -9 appeared to be localized to intracellular membranes. NHX-3 showed highest abundance in the hypodermis with additional expression found in the uterine cells and spermathecal junction cells. NHX-5 occurred primarily in neuronal cell bodies. NHX-8 is localized to the seam cells, but also to the pharyngeal muscles, the pharyngeal-intestinal and intestinal-rectal valve cells. The authors further demonstrated that NHX-9 is targeted to the excretory cell. In a recent study it was suggested that *C. elegans* excretes at least part of its nitrogenous waste in form of ammonia across the hypodermis mediated by the acidification of the apical unstirred boundary layer (Adlimoghaddam et al. 2015).

The aim of the current study was to explore whether NHX-transporters in *C. elegans* play a role in hypodermal H^+ secretion, Na^+ uptake, and ammonia excretion, employing the scanning ion-selective microelectrode technique (SIET) and whole animal excretion experiments. In addition, changes of NHX expression levels were monitored upon physiological stressors such as feeding (elevated internal ammonia loads), starvation, exposure to elevated external ammonia levels, as well as high and low environmental pH regimes.

Materials and Methods

Nematode cultivation

The *Caenorhabditis elegans* strain (N2) employed in this investigation was obtained from the Caenorhabditis Genetics Center (CGC, University of Minnesota, Minneapolis). Worms were maintained in the laboratory at 16°C on Nematode Growth Medium (NGM) seeded as a food source with *E. coli* OP50 according to the standard methods described by Brenner (Brenner 1974). After five days of incubation, chunks of gravid worms on NGM were transferred to freshly seeded NGM plates for revitalization of the animals (Hope 1999). After an incubation period of two days at 16ºC, animals were washed from the plates with M9 buffer (in mmol l^{-1}: 22 KH_2PO_4, 43.5 Na_2HPO_4, 85.54 NaCl, and 3 $MgSO_4$, pH 7) and transferred aseptically into 250 mL of liquid medium as previously described (Adlimoghaddam et al. 2015) using "heat killed" (100°C, 1h) *E. coli* OP50 as a food source. If not noted otherwise, worms starved for 24 hours were used in subsequent experiments to avoid physiological effects and changes in gene-expression patterns related to feeding and corresponding increased internal ammonia loads. All experiments on living worms were performed at room temperature (RT, 22 °C).

Ammonia excretion experiments

In this series of short-term experiments (2 hour treatment), ammonia excretion rates were determined under the influence of amiloride and EIPA (amyloide- and 5-(N-Ethyl-N-isopropyl) amiloride). Worms (8 mL) from the liquid culture were washed twice with non-buffered/control medium (mmol l^{-1}): 129 NaCl, 22 KCl, 1 $MgSO_4$, adjusted to pH 7) followed by a centrifugation step (188 x g, 2 min). Worms of a combined fresh weight of approximately 0.15 - 0.2 g were then exposed to either the control medium or an inhibitor-enriched control medium (pH 7) for 2

hours. Drugs were used at the following concentrations (µmol l^{-1}): 10 and 100 amiloride and 1, 5, 10, 50, 100, and 500 EIPA. EIPA was dissolved in dimethyl sulfoxide (DMSO) at a final concentration of 0.5%. DMSO (0.5%) was also added to the respective control solutions. During the 2 hour incubation period, worms were agitated at 200 rpm at room temperature. At the end of this experimental period, worms were pelleted by centrifugation (188 x g, 3 min) and checked for survival under a microscope. After determining the fresh weight of worms, the supernatants of control media and inhibitor-enriched media were collected. All samples were immediately frozen at -80°C for subsequent ammonia measurement of ammonia concentrations.

Determination of ammonia concentrations

Ammonia concentrations in the samples were determined by means of a gas sensitive NH_3 electrode (Thermo Orion, Beverly, USA) connected to an mV/pH meter as described in detail in previous studies (Weihrauch et al. 1998; Adlimoghaddam et al. 2015).

Determination of body pH

In this set of long-term experiments, body pH was investigated in fed and starved worms as well as in worms exposed to either 1 mmol l^{-1} NH_4Cl (HEA), pH 5.5 and pH 8.0. Approximately 0.15-0.2 g of worms from the liquid culture were washed 2 times and subsequently acclimated for 24 hour to the following solutions: a) control media adjusted to pH 7.0 enriched with "heat killed" *E. coli* OP50 (fed worms); b) control media adjusted to pH 7.0 (no food source, starved worms). Additionally, worms were exposed for 48 hours to c) control media adjusted to pH 7.0 enriched with 1 mmol l^{-1} NH_4Cl; d) control media adjusted to pH 5.5 with 5 mmol l^{-1} 2-(N- morpholino) ethanesulfonic acid (MES); e) control media adjusted to pH

8.0 with 5 mmol l^{-1} tris (hydroxymethyl) aminomethane hydrochloride (Tris-HCL). For treatments c, d and e the media were replaced after 24 hours of incubation so that there was no food source in the last 24 hours. At the end of the treatments, worms were washed twice, pelleted and, after determination of the fresh weight, transferred to a small glass beaker containing 4 mL of millipore water (pH 7.3), and homogenized on ice for 20 s using a polytron homogenizer (AHS, Pro Scientific, Oxford, CT, USA). The homogenized samples were then centrifuged (188 x g, 2 min) and the pH of supernatants was determined using a digital pH meter.

Quantitative PCR:

For this series of experiments animals were treated as described in the preceding section. At the end of each treatment, RNA was extracted from pelleted worms (0.15 – 0.2g) under RNase-free conditions using the RNeasy plus Mini Kit (Qiagen Inc, Mississauga, Ontario, Canada). RNA was then quantified spectrophotometrically (Thermo Fisher Scientific, MA, USA). Following DNase I treatment (Invitrogen, Carlsbad, CA, USA), RNA samples were then checked for DNA contamination by high cycle polymerase chain reaction (PCR) utilizing the primer pair CeActin F/R (Table 1). For cDNA synthesis, 0.3 µg DNased RNA (DNA free) was transcribed using Superscript II reverse transcriptase and oligo-dT primers (iScript™ cDNA Synthesis Kit, Biorad, Mississauga, Ontario, Canada). The quality of cDNA samples was verified by PCR (CeActin F/R) and post run gel visualization.

All primers employed in qPCR were designed based on published sequences as indicated in Table 1. PCR protocols for each employed primer pair were optimized in order to gain a single amplicon of the predicted size (data not shown). All PCR products of all target genes were gel purified (The E.Z.N.A.® gel extraction kit, Omega Bio-Tek, Norcross, Georgia, USA) and

subsequently evaluated for correctness by sequencing (Robarts Research Institute, London, Ontario, Canada).

For quantitative PCR (Miniopticon, Biorad, Mississauga, Ontario, Canada) standard curves of each target gene were generated employing a dilution series of known quantities (10^{+4}, 10^{+3}, 10^{+2}, 10^{+1}, 10^{+0}, 10^{-1} fg DNA) of the respective purified PCR product (QIAquick Gel Extraction Kit, Qiagen Inc, Mississauga, Ontario, Canada). A minimum R^2 value of 0.98 was required for the standard curve. Real-time PCR assays contained a total volume of 15 µL using SSoFast^{TM} EvaGreen supermix (Biorad, Mississauga, Ontario, Canada). After each run a melting curve analysis was performed to verify single product PCR reaction.

SIET

Worms were bathed in moderately hard reconstituted water (MHRW) (Khanna et al. 1997) for measurements of H^+ and Na^+ fluxes. For H^+ flux measurements, MHRW contained (in mmol l^{-1}): 1 NaCl, 1 $NaHCO_3$, 0.3 $CaCl_2$ and 0.1 KCl. For Na^+ flux measurements, NaCl and $NaHCO_3$ were reduced to 0.5 and 0.6 mmol l^{-1}, respectively, to facilitate detection of Na^+ concentration gradients, as described below.

Fluxes of Na^+ and H^+ were measured using SIET. Levamisole (0.5 mmol l^{-1}) was added to all media to minimize worm movements during SIET measurements, as described previously (Adlimoghaddam et al. 2014). Transport of Na^+ or H^+ into or out of the nematode creates gradients in the activities of these ions in the unstirred layer ('boundary layer') near the surface of the hypodermis. Gradients were measured with Na^+-selective and H^+-selective microelectrodes positioned at two points within the unstirred layer. The use of a self-referencing microelectrode permits detection of unstirred layer gradients as small as 0.04% of the

concentration in the bulk solution (*i.e.* outside of the unstirred layer). The microelectrode was moved perpendicular to the worm surface between two positions separated by 50 μm at each measurement site. It was first moved to the inner position within 5 μm of the worm surface. The microelectrode then remained stationary during a 4 s wait period to allow ion gradients near the tissue to re-establish after the localized stirring during the movement period. No data were collected during the wait period. Lastly, the microelectrode voltage was recorded for 0.5 s during the sampling period. The microelectrode was then moved to the other extreme of the 50 μm excursion, perpendicular to the long axis of the worm, followed by another wait and sample period. Each move, wait and sample cycle at each extreme of microelectrode excursion was complete in <5 s. Voltage measurement at both extremes of microelectrode excursion thus required a total of ~10 s and three replicate measurements at each site could thus be completed in <30 s. Voltage measurements taken at the limits of the excursion were used to calculate a mean voltage difference over the excursion distance of the microelectrode. This differential signal was then converted into a Na^+ or H^+ activity difference using standard microelectrode calibration curves that related voltage output to Na^+ or H^+ activity in MHRW. The resultant ion activity gradients were then used to calculate the ion flux, using the Fick equation: $J = D\ \Delta C/\Delta X$, where J is the flux (mol cm^{-2} s^{-1}), D is the diffusion coefficient (cm^2 s^{-1}), ΔC is the concentration gradient (mols cm^{-3}) and ΔX is the distance between the two points (cm). Ion-selective microelectrodes were moved in the X, Y and Z planes by a system of computer-controlled stepper motors. Images of the preparation from a CCD camera mounted on the Zeiss Axiovert microscope were captured by a frame-grabber and the fluxes were overlayed as vectors on the image, permitting spatial differences in ion flux to be shown. SIET measurements were made with hardware from Applicable Electronics (Forestdale, MA, USA). Automated Scanning Electrode Technique

(ASET) software (version 2.0; Science Wares, Falmouth, MA, USA) was used to automate microelectrode positioning, microelectrode voltage recording, and image capture.

Phylogenetic analysis

The CPA1 and CPA2 protein data set contained 33 full length cDNA sequences. Amino acid sequences were aligned by MUSCLE alignment in MEGA 5. Phylogenetic analysis of MUSCLE aligned sequences was done in MEGA 5 using maximum likelihood method with the Jones-Taylor-Thornton + four categories of gamma substitution rates + invariable sites model and Nearest Neighbor Interchange (NNI) Heuristic Method. Bootstrap values were determined from 1000 bootstrap replicates.

Chemicals

All chemicals were obtained from either Sigma-Aldrich (St. Louis, MO, USA) or Thermo Fisher Scientific (MA, USA) unless reported otherwise.

Statistics

With the exception of ion-flux experiments where individual worms were employed (SIET), each N-value represents the combined pool of worms with a mass of approximately 0.15-0.2 g. Values are given as the mean ± standard error of the mean (s.e.m.). The software PAST3 (http://palaeo-electronica.org/2001_1/past/issue1_01.htm; Hammer et al., 2001) was employed for all statistical analysis. Statistical tests performed included Student's t-tests for comparing two means and one-way ANOVA followed by Tukeys post-hoc tests for comparing more than two means. Alternatively, when data were not normally distributed (before and after

log-transformation) and/or homogeneity of variance was not given, the Kruskal-Wallis-Test was applied with post-hoc Mann-Whitney pairwise comparisons. P-values ≤ 0.05 were considered statistically significant. The statistical method employed in each particular experiment is given in the respective figure legends.

Results

As seen in figure 1, an amino acid sequence alignment revealed that all NHX-isoforms in *C. elegans* contain the typical NHE amiloride binding motif, with the exception that at position 9 in NHX-2 and NHX-6b a leucine is replaced by an isoleucine. There is a 100% match of the relevant amino acid leucine at position 3 within that motif for the amiloride-sensitive human NHE-1 and NHX-1, - 8a, -9a as well as the hypodermally expressed NHX-3a.

Na^+ and H^+ fluxes across the hypodermis of C. elegans

To evaluate the participation of NHX proteins in hypodermal Na^+-uptake and H^+ excretion, ion fluxes across the hypodermis were measured by SIET in control N2 medium and in the presence of 100 µmol l^{-1} amiloride or EIPA. The current study showed that regions of the hypodermis > 100 µm posterior to the excretory pore in wild-type worms (N2) take up Na^+ at a rate of 20.8 ± 1.3 pmol cm^{-2} s^{-1} (N=6), which is ~ 7 times greater than the observed rate of H^+ excretion (2.97 ± 0.21 pmol cm^{-2} s^{-1}, N=5) (Fig. 2). Application of 100 µmol l^{-1} amiloride reduced Na^+ uptake and H^+ secretion by ca. 60% and 42%, respectively. In contrast, the application of 100 µmol l^{-1} EIPA had no effect on the H^+ flux rate (Fig. 3).

Effects of amiloride and EIPA on ammonia excretion

To determine the participation of NHX proteins in the ammonia excretion process, various concentrations of either amiloride or EIPA were applied and ammonia excretion rates of whole worms monitored. While ammonia excretion rates decreased significantly by ca. 23% and 40% after application of 10 and 100 µmol l^{-1} amiloride, respectively, exposure to various concentrations of EIPA (1 to 500 µmol l^{-1}) caused no inhibition of the flux (Fig. 4).

Effects of starvation, high environmental ammonia (HEA), high pH and low pH on gene expression levels of NHX isoforms.

To evaluate responses of all NHX isoforms to internal and external stressors, changes of mRNA expression levels were assessed in worms which were either starved or exposed to elevated environmental ammonia (1 mmol L^{-1}, HEA), high pH (8.0) and low pH (5.5).

In fed worms, mRNAs of the nine NHX isoforms expressed in *C. elegans* showed different expression levels when compared to each other. Highest mRNA expression levels were detected for NHX-1 and NHX-4 followed by moderate expression levels for NHX-2, -5, -7, low levels for NHX-3 and -9, and lowest levels for NHX-6 and -8 (Table 2).

When animals were deprived of food for 24 hours a moderate to strong down-regulation of NHX-2, -3, -4, and -5 was detected. Also, while mRNA expression levels NHX-1, -6, -7, and -8 displayed no changes after starvation, mRNA expression level of NHX-9 increased approximately 2-fold (Fig. 5A). In addition, body pH decreased by 0.17 units after starvation (Table 3).

To avoid effects from internal ammonia loads due to protein catabolism, only starved animals were employed in the following three series of experiments (HEA, low and high pH

regimes). After a 2 day exposure to 1 mmol l^{-1} NH_4Cl, mRNA expression levels of the intestinal NHX-2 increased and there was a trend towards an increase in neuronal NHX-5 (p= 0.06). By contrast, there was a decrease in expression of hypodermal NHX-3 and the housekeeping NHX-4. A trend towards reduced expression was also seen for the basolaterally expressed intestinal NHX-6 (Fig. 5B). Exposure to HEA had no effect on body pH (Table 3).

A 48 hour exposure to a low environmental pH (5.5) was associated with an up-regulation of ca. 4-, 3-, and 2-fold for NHX-2, -3 and -5, respectively, while NHX-9, which is localized to the excretory cell, was partially down-regulated. A strong down-regulation was also found for NHX-4 (Fig. 5C). The body pH decreased by 0.28 units after exposure to a low environmental pH (Table 3).

When animals were exposed for 48 hours to pH 8, NHX-2, 3, 5, 6, 7, and -8 showed an up-regulation, while, similar to the findings under low pH exposure, NHX-4 and -9 were down-regulated (Fig. 5D). In contrast to the low pH treatment and starvation, body pH did not change after exposure to pH 8 (Table 3).

Discussion

Effect of EIPA and amiloride on ammonia excretion and hypodermal Na^+ and H^+ fluxes.

The scanning ion-selective electrode technique (SIET) permits direct measurements of Na^+ and H^+ fluxes across the hypodermis of the minute nematode *C. elegans*. In the current study we found Na^+ uptake and H^+ secretion over the hypodermis, suggesting an apically localized V-ATPase that drives indirectly apical NH_3 excretion *via* RHR-2 (Adlimoghaddam et al. 2016), and Na^+ uptake via Na^+ channels as proposed e.g. in the gills of strong hyper-regulating crabs or branchial PNA^- cells in rainbow trout gills (Larsen et al. 2014). Alternatively, participation of an

329 apically-localized cation/proton exchanger in these transport processes might be considered. It is
330 noteworthy, that Na^+ uptake rates were approximately 9-times greater than H^+ secretion rates,
331 indicating that additional Na^+ uptake mechanism, must be in place under this scenario. However,
332 the strong presence of NHX-1 and -3 in the hypodermis and their identified/speculated plasma
333 membrane localization in *C. elegans* led to the assumption that these two transporters are
334 potential candidate transporters contributing to the measured cation fluxes (Nehrke and Melvin
335 2002) (see also figure 6). Our sequence analysis revealed that the hypodermally expressed NHX-
336 1 and NHX-3 exhibit the conserved amiloride binding motif. Furthermore, both NHXs contain,
337 as in the mammalian NHE-1, a leucine in the third position of the amiloride binding motif (Fig.
338 1), an amino acid critical for amiloride sensitivity (Counillon et al. 1993). Consequently, an
339 inhibition of the Na^+, H^+, and possibly ammonia fluxes was expected after the application of
340 inhibitory agents. After exposure to relatively high concentrations (100 µmol l^{-1}) of EIPA, an
341 amiloride derivate and potent inhibitor of NHEs in vertebrate and invertebrate epithelia
342 (Kleyman and Cragoe 1988; Blaesse et al. 2010), no inhibition of the hypodermal H^+ flux and
343 whole animal ammonia excretion was observed. Although in need for experimental
344 confirmation, it is fairly unlikely that hypodermal NHX-1 and NHX-3 are not EIPA sensitive as,
345 in contrast to the EIPA un-sensitive housekeeping NHX-4 (Nehrke and Melvin 2002), both
346 contain a leucine in the third position within the amiloride binding motif. It is more likely that
347 both NHX-1 and NHX-3 are simply not involved in apical H^+ and ammonia excretion. As
348 mentioned in the introduction, NHX-3 is localized primarily to intracellular membranes, while
349 the cellular localization of NHX-1 is still unknown. In contrast to the absence of effects of EIPA
350 (100 µmol l^{-1}), amiloride caused a decrease not only in hypodermal H^+ and Na^+ fluxes, but also
351 in whole animal ammonia excretion rates (Fig. 4), even at a low dose of 10 µmol l^{-1}. Since EIPA

is the more specific and more potent inhibitor of NHEs, compared to amiloride, it seems likely that the effects seen with amiloride are due to a partial or full blockage of apical Na^+ channels as this inhibitor functions at low doses as a very potent Na^+ channel blocker, (Kleyman and Cragoe 1988; Blaesse et al. 2010). How can a blockage of apical Na^+ uptake influence ammonia excretion rates?

A reduced Na^+ uptake would have an inhibitory effect on the Na^+/K^+-ATPase due to the consequent reduction in intracellular availability of Na^+ as a substrate. As recently suggested, the Na^+/K^+-ATPase is most likely a key player in hypodermal ammonia transport because it accepts not only K^+, but instead also NH_4^+ as a substrate. (Adlimoghaddam et al. 2015). The pump is therefore responsible, for the transport of ammonia from the body fluids into the hypodermal syncytium. Such a role of the Na^+/K^+-ATPase in ammonia transport processes has been described for many vertebrate and invertebrate epithelia (Larsen et al. 2014). Another possibility for the observed changes in transport rates could be that a blockage of the Na^+ ion pathway over the apical membrane of the hypodermis caused a hyperpolarization of the syncytium, as observed for epithelial cells in the frog skin. Here, the inhibition of the Na^+ entry by apical application of amiloride caused a hyperpolarization of the epithelial cells and consequently also an inhibition of the net H^+ efflux (Harvey and Ehrenfeld 1988). Assuming also in *C. elegans* the presence of NH_4^+ and H^+ conductive pathways in the apical membrane of the syncytium, e.g. K^+ channels, AMTs (ammonium transporters) and V-ATPase, reduced cation transport rates are expected due to a less favorable electrochemical gradient.

Effects of starvation and high environmental ammonia (HEA) on mRNA expression levels of epithelial NHX-2, -3 and -9.

As mentioned in the introduction, NHEs play a crucial role in pH homeostasis (Orlowski and Grinstein 2004). Therefore it is most likely that also the NHX-transporters in the nematode play a role in pH homeostasis under various pH challenging conditions such exposure to high and low environmental pH regimes and internal or external ammonia loads. The following discussion focuses on NHX-2, -3 and -9 expressed in the intestine, hypodermis and excretory cell, respectively, and found within the CPA1 subcluster of transporters to be localized in recycling vesicles or residential in plasma membranes (Fig. 6).

Feeding

An earlier study showed that fed *C. elegans* exhibited 3-fold higher ammonia excretion rates compared to starved animals, likely due to an elevated internal ammonia load caused by protein catabolism (Adlimoghaddam et al. 2015). Feeding was also correlated with an up-regulation of NHX isoforms highly abundant in epithelia of the intestine (NHX-2) and hypodermis (NHX-3). Participation of the intestinal expressed NHX-2 in digestive related electrolyte transport during defecation was also suggested by early by Allman and co-workers (Allman et al. 2009).

In contrast, transcripts of NHX-9, abundant in the excretory cell, were down-regulated during feeding. This suggests that these epithelial transporters are involved in regulating feeding-related pH variations of the body fluids, but may also play a role in ammonia excretion. NHEs have been linked to ammonia transport through their capacity to build up a transmembrane pH gradient and thereby also a ΔP_{NH3} (Weihrauch et al. 2012; Shih et al. 2012; Wright and Wood 2009), thus promoting ammonia trapping. Localized in the apical membrane of the intestine, NHX-2 is likely, together with an apically localized V-ATPase (Allman et al. 2009), responsible

for acidifying the unstirred apical layer in the gut lumen, creating thereby a ΔP_{NH3}. NHX-3 on the other hand, is primarily located intracellularly, (Nehrke and Melvin 2002), possibly in intracellular vesicles recycling to the plasma membrane similar to the mammalian NHE3 (Brett et al. 2005) as our sequence analysis implies (Fig. 6). A vesicular NHX-3 could acidify the compartmental lumen, trapping thereby ammonia in form of NH_4^+. Indeed, a vesicular ammonia excretion was suggested in an earlier study as inhibitory effects on excretion were observed after the application of colchicine (Adlimoghaddam et al. 2015). Members of the CPA2 subfamily, the electrogenic NHAs, do not contain an amiloride binding motif and cluster distinctively to the NHEs (Fig. 6). NHAs have been correlated to acid-base regulatory mechanisms in insects (Rheault et al. 2007; Weihrauch and O'Donnell 2015; Day et al. 2008), while future studies must show their role in the nematoda.

Exposure to high environmental ammonia (HEA)

A recent study revealed that exposure to HEA (1 mmol l^{-1}) caused a 7 fold increase in body ammonia but also a doubling of the ammonia excretion rate (Adlimoghaddam et al. 2015). In the current study it was observed that body pH was not affected in worms after a 2 day exposure to HEA. However, under this stress, NHX-2 mRNA levels increased more than 3.5 fold, indicating that this transporter is involved in intestinal ammonia excretion and/or the regulation of acid-base homeostasis after HEA exposure.

After a 2 day HEA exposure NHX-3 was slightly down-regulated, indicating a minor importance for this transporter in the ammonia excretion process under this condition. Further, due to the lack of response, NHX-9 seems not to play a significant role in the ammonia handling processes in the excretory cell. The potential importance of NHX-2 in intestinal ammonia

handling is further underlined by the overall high abundance of its mRNA, which is approximately 10 times greater compared to NHX-3 (Table 2).

The effects of high and low environmental pH on NHX mRNA expression levels

Exposure to pH 5.5

Exposure to an environmental pH of 5.5 had significant effects on the mRNA expression levels of NHX transporters localized in the epithelium (NHX-2, -3, -4 and -9). The corresponding body pH was 6.35 and thus not different from values found in the control (also starved) animals (Table 3). While the up-regulation of NHX-2 and -3 indicates an involvement in the protective acid secretion process, the observed slight down-regulation of NHX-9 upon low pH stress is more difficult to interpret and awaits more investigations towards its general role in the excretory cell.

The severe down-regulation of the housekeeping gene NHX-4 (Fig. 5C) is, however, also puzzling, since its basolateral localization should protect the cells from detrimental effects due to acidification. In epithelial cells however, a lower abundance of this transporter could mean a lower H^+ back-flow from the cells into the body fluids, and thereby potentially enhance H^+ secretion. Again, all these assumptions are at this moment speculative as experimental proof is lacking.

Up-regulation of NHX-5, in contrast, suggests a protective role of this transporter in the neuronal cells, in spite of its cytoplasmic, rather than plasma membrane predicted localization (Fig. 6).

Exposure to pH 8

When exposed to an elevated external pH of 8, body pH increased by approximately 0.2 units when compared to the respective control values in starved animals (Table 3).

Again puzzling, changes in gene expression levels of the NHX isoforms were very similar, with the same direction but even more pronounced when compared to the effects seen after a low pH exposure. In addition, an up-regulation of the intestinal NHX-6 and -7 isoforms and also the NHX-8 (seam cells) isoforms was seen in response to high pH stress. NHX-6 and -7 are localized to the basolateral membrane, promoting possibly a compensatory H^+ influx into the body fluids. Overall, the results from the pH experiments are not conclusive, but they do underline the general physiological importance in acid-base homeostasis of basically all NHX transporters. It is clear that more experiments need to be undertaken to further our understanding in the nematode's acid-base regulation and the particular role of each member of the CPA1 sub-family. This includes functional transport studies as well as the determination if K_i values towards amiloride and its derivatives.

Conclusion

The current study provides new information regarding the role of NHXs in the acid base homeostasis in the genetic model system *C. elegans*. A most recent study on this worm suggested that ammonia excretion across the hypodermis involves a basal Na^+/K^+-ATPase, a vesicular microtubule-dependent transport mechanism, and an ammonia trapping mechanism over the apical membrane, which is promoted by an acidification of the apical unstirred boundary layer (Adlimoghaddam et al. 2015) .

Unexpectedly, it was observed that NHXs are likely not involved in H^+ secretion and ammonia excretion over the apical membrane of the hypodermis in *C. elegans*, suggesting a lack of expression in this membrane. By contrast, our results point rather to a role of an apically localized Na^+ channel in both processes, which can be inhibited by low concentrations of amiloride. If this holds true in future studies, the Na^+ uptake mechanism in the soil nematode *C. elegans* may be comparable to that found in the osmoregulatory tissues found in freshwater living animals such as amphibians and crustaceans (Henry et al. 2012; Klein et al. 1997). Gene-expression analysis revealed further that, in contrast to the NHX isoforms expressed in the hypodermis, or NHX-9, which is localized in the excretory cell, the isoform localized to the apical membrane of the intestine (NHX-2) seems to be important in acid-base homeostasis and probably also in elimination of metabolic ammonia.

Acknowledgements

This work was supported by NSERC Canada Discovery Grants to D.W., and M.J. O'D.. D. W. is also supported by Canada Foundation for Innovation.

5. Literature

Adlimoghaddam A, Boeckstaens M, Marini AM, Treberg JR, Brassinga A-K, Weihrauch D (2015) Ammonia excretion in *Caenorhabditis elegans*: mechanism and evidence of ammonia transport of the Rh-protein CeRhr-1. J Exp Biol 218:675-683

Adlimoghaddam A, O'Donnell MJ, Kormish J, Banh S, Treberg JR, Merz D, Weihrauch D (2016) Ammonia excretion in Caenorhabditis elegans: Physiological and molecular characterization of the rhr-2 knock-out mutant. Comp Biochem Physiol A Mol Integr Physiol 195:46-54. doi:10.1016/j.cbpa.2016.02.003

Adlimoghaddam A, Weihrauch D, O'Donnell MJ (2014) Localization of K^+, H^+, Na^+ and Ca^{2+} fluxes to the excretory pore in *Caenorhabditis elegans*: application of scanning ion-selective microelectrodes. The Journal of experimental biology 217 (23):4119-4122

493 Allman E, Johnson D, Nehrke K (2009) Loss of the apical V-ATPase a-subunit VHA-6 prevents
494 acidification of the intestinal lumen during a rhythmic behavior in C. elegans. Am J
495 Physiol Cell Physiol 297 (5):C1071-1081. doi:10.1152/ajpcell.00284.2009
496 Blaesse AK, Broehan G, Meyer H, Merzendorfer H, Weihrauch D (2010) Ammonia uptake in
497 Manduca sexta midgut is mediated by an amiloride sensitive cation/proton exchanger:
498 Transport studies and mRNA expression analysis of NHE7, 9, NHE8, and V-ATPase
499 (subunit D). Comp Biochem Physiol A Mol Integr Physiol 157 (4):364-376. doi:S1095-
500 6433(10)00447-2 [pii]
501 10.1016/j.cbpa.2010.08.004
502 Brenner S (1974) The genetics of Caenorhabditis elegans. Genetics 77 (1):71-94
503 Brett CL, Donowitz M, Rao R (2005) Evolutionary origins of eukaryotic sodium/proton
504 exchangers. Am J Physiol Cell Physiol 288 (2):C223-239.
505 doi:10.1152/ajpcell.00360.2004
506 Counillon L, Franchi A, Pouyssegur J (1993) A point mutation of the Na+/H+ exchanger gene
507 (NHE1) and amplification of the mutated allele confer amiloride resistance upon chronic
508 acidosis. Proc Natl Acad Sci U S A 90 (10):4508-4512
509 Counillon L, Noel J, Reithmeier RA, Pouyssegur J (1997) Random mutagenesis reveals a novel
510 site involved in inhibitor interaction within the fourth transmembrane segment of the
511 Na+/H+ exchanger-1. Biochemistry 36 (10):2951-2959
512 Day JP, Wan S, Allan AK, Kean L, Davies SA, Gray JV, Dow JA (2008) Identification of two
513 partners from the bacterial Kef exchanger family for the apical plasma membrane V-
514 ATPase of Metazoa. J Cell Sci 121 (Pt 15):2612-2619. doi:10.1242/jcs.033084
515 Edwards SL, Tse CM, Toop T (1999) Immunolocalisation of NHE3-like immunoreactivity in the
516 gills of the rainbow trout (Oncorhynchus mykiss) and the blue-throated wrasse
517 (Pseudolabrus tetrious). Journal of anatomy 195 (Pt 3):465-469
518 Harvey BJ, Ehrenfeld J (1988) Epithelial pH and ion transport regulation by proton pumps and
519 exchangers. Ciba Foundation symposium 139:139-164
520 Henry RP, Lucu C, Onken H, Weihrauch D (2012) Multiple functions of the crustacean gill:
521 osmotic/ionic regulation, acid-base balance, ammonia excretion, and bioaccumulation of
522 toxic metals. Front Physiol 3:431. doi:10.3389/fphys.2012.00431
523 Hirata T, Kaneko T, Ono T, Nakazato T, Furukawa N, Hasegawa S, Wakabayashi S, Shigekawa
524 M, Chang MH, Romero MF, Hirose S (2003) Mechanism of acid adaptation of a fish
525 living in a pH 3.5 lake. Am J Physiol Regul Integr Comp Physiol 284 (5):R1199-1212.
526 doi:10.1152/ajpregu.00267.2002
527 Hope IA (1999) C. elegans: A Practical Approach. Oxford University Press, Oxford,
528 Ivanis G, Esbaugh AJ, Perry SF (2008) Branchial expression and localization of SLC9A2 and
529 SLC9A3 sodium/hydrogen exchangers and their possible role in acid-base regulation in
530 freshwater rainbow trout (Oncorhynchus mykiss). J Exp Biol 211 (Pt 15):2467-2477.
531 doi:211/15/2467 [pii]
532 10.1242/jeb.017491
533 Khanna N, Cressman III C, Tatara C, Williams P (1997) Tolerance of the nematode
534 *Caenorhabditis elegans* to pH, salinity, and hardness in aquatic media. Archives of
535 environmental contamination and toxicology 32 (1):110-114
536 Kinsella JL, Aronson PS (1981) Interaction of NH4+ and Li+ with the renal microvillus
537 membrane Na+-H+ exchanger. Am J Physiol 241 (5):C220-226

Klein U, Timme M, Zeiske W, Ehrenfeld J (1997) The H+ pump in frog skin (Rana esculenta): identification and localization of a V-ATPase. J Membr Biol 157 (2):117-126
Kleyman TR, Cragoe EJ, Jr. (1988) Amiloride and its analogs as tools in the study of ion transport. J Membr Biol 105 (1):1-21
Larsen EH, Deaton LE, Onken H, O'Donnell M, Grosell M, Dantzler WH, Weihrauch D (2014) Osmoregulation and excretion. Comprehensive Physiology 4 (2):405-573. doi:10.1002/cphy.c130004
Murtazina R, Booth BJ, Bullis BL, Singh DN, Fliegel L (2001) Functional analysis of polar amino-acid residues in membrane associated regions of the NHE1 isoform of the mammalian Na+/H+ exchanger. Eur J Biochem 268 (17):4674-4685. doi:ejb2391 [pii]
Nagami GT (1988) Luminal secretion of ammonia in the mouse proximal tubule perfused in vitro. J Clin Invest 81 (1):159-164. doi:10.1172/JCI113287
Nawata CM, Hirose S, Nakada T, Wood CM, Kato A (2010) Rh glycoprotein expression is modulated in pufferfish (Takifugu rubripes) during high environmental ammonia exposure. J Exp Biol 213 (Pt 18):3150-3160. doi:10.1242/jeb.044719
Nehrke K, Melvin JE (2002) The NHX family of Na+-H+ exchangers in Caenorhabditis elegans. J Biol Chem 277 (32):29036-29044. doi:10.1074/jbc.M203200200
Orlowski J, Grinstein S (2004) Diversity of the mammalian sodium/proton exchanger SLC9 gene family. Pflugers Arch 447 (5):549-565. doi:10.1007/s00424-003-1110-3
Piermarini PM, Weihrauch D, Meyer H, Huss M, Beyenbach KW (2009) NHE8 is an intracellular cation/H+ exchanger in renal tubules of the yellow fever mosquito Aedes aegypti. Am J Physiol Renal Physiol 296 (4):F730-750. doi:90564.2008 [pii]
10.1152/ajprenal.90564.2008
Pullikuth AK, Aimanova K, Kang'ethe W, Sanders HR, Gill SS (2006) Molecular characterization of sodium/proton exchanger 3 (NHE3) from the yellow fever vector, Aedes aegypti. J Exp Biol 209 (Pt 18):3529-3544. doi:209/18/3529 [pii]
10.1242/jeb.02419
Randall DJ, Wilson JM, Peng KW, Kok TW, Kuah SS, Chew SF, Lam TJ, Ip YK (1999) The mudskipper, *Periophthalmodon schlosseri*, actively transports NH_4^+ against a concentration gradient. Am J Physiol 277 (6 Pt 2):R1562-1567
Rheault MR, Okech BA, Keen SB, Miller MM, Meleshkevitch EA, Linser PJ, Boudko DY, Harvey WR (2007) Molecular cloning, phylogeny and localization of AgNHA1: the first Na+/H+ antiporter (NHA) from a metazoan, Anopheles gambiae. J Exp Biol 210 (Pt 21):3848-3861. doi:210/21/3848 [pii]
10.1242/jeb.007872
Scott GR, Claiborne JB, Edwards SL, Schulte PM, Wood CM (2005) Gene expression after freshwater transfer in gills and opercular epithelia of killifish: insight into divergent mechanisms of ion transport. J Exp Biol 208 (Pt 14):2719-2729. doi:10.1242/jeb.01688
Shih TH, Horng JL, Liu ST, Hwang PP, Lin LY (2012) Rhcg1 and NHE3b are involved in ammonium-dependent sodium uptake by zebrafish larvae acclimated to low-sodium water. Am J Physiol Regul Integr Comp Physiol 302 (1):R84-93. doi:ajpregu.00318.2011 [pii]
10.1152/ajpregu.00318.2011
Slepkov ER, Rainey JK, Li X, Liu Y, Cheng FJ, Lindhout DA, Sykes BD, Fliegel L (2005) Structural and functional characterization of transmembrane segment IV of the NHE1

583 isoform of the Na+/H+ exchanger. J Biol Chem 280 (18):17863-17872. doi:M409608200
584 [pii]
585 10.1074/jbc.M409608200
586 Slepkov ER, Rainey JK, Sykes BD, Fliegel L (2007) Structural and functional analysis of the
587 Na+/H+ exchanger. Biochem J 401 (3):623-633. doi:BJ20061062 [pii]
588 10.1042/BJ20061062
589 Touret N, Poujeol P, Counillon L (2001) Second-site revertants of a low-sodium-affinity mutant
590 of the Na+/H+ exchanger reveal the participation of TM4 into a highly constrained
591 sodium-binding site. Biochemistry 40 (16):5095-5101. doi:bi0025464 [pii]
592 Towle DW, Rushton ME, Heidysch D, Magnani JJ, Rose MJ, Amstutz A, Jordan MK, Shearer
593 DW, Wu WS (1997) Sodium/proton antiporter in the euryhaline crab *Carcinus maenas*:
594 molecular cloning, expression and tissue distribution. J Exp Biol 200 (Pt 6):1003-1014
595 Towle DW, Weihrauch D (2001) Osmoregulation by gills of euryhaline crabs: molecular
596 analysis of transporter. Am Zool 41:770-780
597 Tse M, Levine S, Yun C, Brant S, Pouyssegur J, Donowitz M (1993) The mammalian Na+/H+
598 exchanger gene family--initial structure/function studies. J Am Soc Nephrol 4 (4):969-
599 975
600 Wakabayashi S, Fafournoux P, Sardet C, Pouyssegur J (1992) The Na+/H+ antiporter
601 cytoplasmic domain mediates growth factor signals and controls "H(+)-sensing". Proc
602 Natl Acad Sci U S A 89 (6):2424-2428
603 Wakabayashi S, Pang T, Su X, Shigekawa M (2000) A novel topology model of the human
604 Na(+)/H(+) exchanger isoform 1. J Biol Chem 275 (11):7942-7949
605 Weihrauch D (2006) Active ammonia absorption in the midgut of the Tobacco hornworm
606 Manduca sexta L.: Transport studies and mRNA expression analysis of a Rhesus-like
607 ammonia transporter. Insect Biochem Mol Biol 36 (10):808-821
608 Weihrauch D, Becker W, Postel U, Riestenpatt S, Siebers D (1998) Active excretion of ammonia
609 across the gills of the shore crab *Carcinus maenas* and its relation to osmoregulatory ion
610 uptake. J Comp Physiol [B] 168:364-376
611 Weihrauch D, Chan AC, Meyer H, Doring C, Sourial MM, O'Donnell MJ (2012) Ammonia
612 excretion in the freshwater planarian Schmidtea mediterranea. J Exp Biol 215:3242-3253.
613 doi:jeb.067942 [pii]
614 10.1242/jeb.067942
615 Weihrauch D, O'Donnell MJ (2015) Links between Osmoregulation and Nitrogen-Excretion in
616 Insects and Crustaceans. Integr Comp Biol 55 (5):816-829. doi:10.1093/icb/icv013
617 Weiner ID, Hamm LL (2007) Molecular mechanisms of renal ammonia transport. Annu Rev
618 Physiol 69:317-340. doi:10.1146/annurev.physiol.69.040705.142215
619 Wieczorek H, Beyenbach KW, Huss M, Vitavska O (2009) Vacuolar-type proton pumps in
620 insect epithelia. J Exp Biol 212 (Pt 11):1611-1619. doi:212/11/1611 [pii]
621 10.1242/jeb.030007
622 Wilson JM, Laurent P, Tufts BL, Benos DJ, Donowitz M, Vogl AW, Randall DJ (2000) NaCl
623 uptake by the branchial epithelium in freshwater teleost fish: an immunological approach
624 to ion-transport protein localization. J Exp Biol 203 (Pt 15):2279-2296
625 Wright PA, Wood CM (2009) A new paradigm for ammonia excretion in aquatic animals: role of
626 Rhesus (Rh) glycoproteins. J Exp Biol 212 (Pt 15):2303-2312. doi:212/15/2303 [pii]
627 10.1242/jeb.023085

Zachos NC, Tse M, Donowitz M (2005) Molecular physiology of intestinal Na+/H+ exchange. Annu Rev Physiol 67:411-443. doi:10.1146/annurev.physiol.67.031103.153004

Table 1: Primers employed in PCR targeting Na^+/H^+ exchangers (NHX-1, NHX-2, NHX-3 isoform a, NHX-4 isoform a, NHX-5 isoform a, NHX-6 isoform a, NHX-7, NHX-8 isoform b, NHX-9 isoform b) from the nematode, *Caenorhabditis elegans*.

Primer	**Nucleotide sequence (5'→3')**	**Annealing Temp. (ºC)**	**Product size (bp)**	**GenBank Acc. #**
Na^+/H^+ exchanger				
CeNHX-1 F	AAAACAAAGTCGACAAATGG			
CeNHX-1 R	CCCGTTCCTCCTATA CTTGA	58	180	NM_078221.5
CeNHX-2 F	AAGACATTGCCGGTTTCAAG			
CeNHX-2 R	TCCACGTGCAATCTTCTTTG	60	179	NM_063213.4
CeNHX-3 F	GCGGGTCAACGTGGTCATTA			
CeNHX-3 R	TGTGGCGTCGAAGCTTTGTC	60	110	NM_001028564.2
CeNHX-4 F	GGATTTGCCGGTGTGTTCAT			
CeNHX-4 R	TGCCCAGTTTCAGCAAGGA	60	114	NM_001029391.2
CeNHX-5 F	AAGCCGACTTGTTTGCGTTA			
CeNHX-5 R	CGCGTTCATACATCCAATCA	57	200	NM_001029549.2
CeNHX-6 F	CCTCTACCGGATGTTCCTGA			
CeNHX-6 R	TGAAGACGCAGTTGAGGATG	58	197	NM_001027043.2
CeNHX-7 F	TTATTGCACTGATTGCCTGC			
CeNHX-7 R	CCGAAACTGCAGAGAACACA	54	207	AF497831.1
CeNHX-8 F	ATCGGGTATCATGGCAATTC			
CeNHX-8 R	CCAGAATATGAGCCACGGT	60	200	NM_001026558.2
CeNHX-9 F	TGGATTATGCAACTGGTGGA			
CeNHX-9 R	TTGCGATTGCTATGATGGAG	60	207	AF497835.1

Table 2: Absolute mRNA expression levels (fg DNA/50 ng total RNA) of NHX isoforms in *C. elegans*. For statistical analysis a Kruskal-Wallis-Test was applied with post-hoc Mann-Whitney pairwise comparisons. Significant differences are indicated by different letters ($p \leq 0.05$).

	NHX-1	NHX-2	NHX-3	NHX-4	NHX-5	NHX-6	NHX-7	NHX-8	NHX-9
Mean	28.5	11.4	0.9	35.6	2.9	0.1	3.2	0.2	1.1
s.e.m.	3.7	3.1	0.1	2.0	0.5	0.02	0.4	0.04	0.2
N	5	5	5	5	5	3	5	5	5
Statistics	a	b	c	a	b	d	b	d	c

Table 3: Body pH of homogenized *C. elegans* cultured in different media. Fed, unbuffered media pH 7; Starved, starved for 24 hours, unbuffered media pH 7; HEA, starved for 24 hours, unbuffered media enriched with 1 mmol l^{-1} NH_4Cl (48 hours), pH 7; pH 5.5, starved for 24 hours, MES buffered media, pH 5.5 (48 hours); pH 8, starved for 24 hours, TRIS buffered media, pH 8 (48 hours). For statistical analysis a Kruskal-Wallis-Test was applied with post-hoc Mann-Whitney pairwise comparisons. Significant differences are indicated by different letters ($p \leq 0.05$).

	Fed	Starved	HEA	pH 5.5	pH 8.0
Mean	6.63	6.46	6.65	6.35	6.67
s.e.m.	0.016	0.022	0.027	0.050	0.023
N	5	5	5	5	5
Statistics	a	b	a	b	a

Figure legends

Figure 1: The conserved amiloride binding motif is indicated in the outer black box. A critical leucine, underlaid in grey within the pocket, renders amiloride sensitivity. Mammalian NHE1 (Orlowski & Grinstein et al., 2004) was shown to be amiloride-sensitive. The diagram was constructed with MultAlign (bioinfo.genopole-toulouse.prd.fr/multalin/ multalin.html). Accession numbers are given in parentheses: *H. sapiens* NHE1 (NP_003038); NHX-1(NM_078221.5); NHX-2 (NM_063213.4); NHX-3a (NM_001028564.2); NHX-4a (NM_001029391.2); NHX-5a (NM_001029549.2); NHX-6b (NM_001027043.2); NHX-7 (AF497831.1); NHX-8a (NM_001026558.2); NHX-9a AF497835.1).

Figure 2: Representative scans showing voltage differences recorded by SIET over the hypodermis for H^+ fluxes (A) and Na^+ fluxes (B) at locations 100 µm or more posterior to the excretory pore of adult *C. elegans*. The length of the arrow corresponds to the mean voltage difference of 3 replicate measurements at each site. Voltage scales are provided in the top right of each panels.

Figure 3: H^+ and Na^+ fluxes over the hypodermis of adult wild type *C. elegans* (N2) under the influence of either 100 µmol l^{-1} amiloride (black bars) or 100 µmol l^{-1} EIPA (gray bar). (A) H^+ efflux; N = 5; (B) Na^+ influx; N = 5-6. Data represent means ± s.e.m. and were analyzed employing one-way ANOVA followed by Tukeys post-hoc tests. Significant differences are indicated by different letters.

687 Figure 4: Ammonia excretion rates of *C. elegans* exposed to various concentrations of
688 EIPA (Panel A; N=6) and amiloride (Panel B; N= 4-5). Control conditions = unbuffered control
689 media (pH=7, open bar). Data represent means ± s.e.m. and were analyzed employing one-way
690 ANOVA followed by Tukeys post-hoc tests. Significant differences are indicated by different
691 letters.
692
693 Figure 5: Changes of mRNA expression levels of NHX-1 to -9 after 1 day starvation
694 (Panel A; N=4-5), 2 day exposure to 1 mmol l^{-1} NH_4Cl (HEA) in starved worms (Panel B; N=4-
695 5), 2 day exposure to pH 5.5 in starved worms (Panel C; N=4-5), and 2 day exposure to pH 8.0
696 in starved worms (Panel D; N=4-5). Absolute mRNA expression levels of respective control
697 animals were set to 1 (open bars) with values measured under the experimental conditions are
698 given as "fold changes" of the respective controls (closed bars). The asterisk (*) indicates
699 significant differences between treatments ($p \leq 0.05$). Data represent means ± s.e.m. and were
700 analyzed employing an unpaired, two-tailed Student's t-test prior to calculation for fold change
701 values.
702
703 Figure 6: Maximum likelihood unrooted tree of members of the CPA superfamily. Numbers
704 beside branches represent bootstrap values from 1000 replicates. The tree branches are drawn to
705 scale, with the scale bar representing the number of amino acid substitutions per site. Based on
706 subcellular localization and function the CPA1 clade (NHEs) can be divided into two subcluster,
707 containing either a) NHEs localized to plasma membranes or submembranous vesicles cycling to
708 the plasma membranes or b) NHEs localized to endomembranes (Golgi or endosomes) (Nehrke
709 and Melvin 2002; Brett et al. 2005; Tse et al. 1993; Piermarini et al. 2009; Ivanis et al. 2008;

Pullikuth et al. 2006). Note, the nomenclature of the mammalian NHEs is not consistent with the nomenclature in *C. elegans*.

Accession numbers are given in parentheses: AeNHE3 (AAM63432.1), AeNHE79 (XP_001654568.1), AeNHE8 (ACJ02512.1), AgNHA1 (ABJ91581), AgNHA2 (XP_312647), CeNHX1 (NP_510622), CeNHX2 (NP_495614), CeNHX3a (NP_001023735), CeNHX4a (NP_001024562), CeNHX5a (NP_001024720), CeNHX6a (NP_001022214), CeNHX7 (AAM18109), CeNHX8a (NP_001021728), CeNHX9a (NP_001023627), CeNHA1 (NP_509724), CeNHA2 (NP_509723), CeNHA3 (NP_507130), CmNHE (AAC26968), DmNHA1 (NP_723224), DmNHA2 (NP_732807), HsNHE1 (NP_003038.2), HsNHE2 (Q9UBY0.1), HsNHE3 (AAI01670), HsNHE4 (NP_001011552), HsNHE5 (Q14940), HsNHE6a (NP_001036002), HsNHE7 (NP_115980), HsNHE8 (Q9Y2E8), HsNHE9 (BAD69592), HsNHA1 (NP_631912), HsNHAmt (NP_849155), MsNHE8 (ABX71221.1), OmNHE (NP_001118167). Abbreviations: Ae, *Aedes aegypti*; Ag, *Anopheles gambia*; Ce, *Caenorhabditis elegans* ; Cm, *Carcinus maenas*; Dm, *Drosophila melanogaster*; Hs, *Homo sapiens*; Ms, *Manduca sexta*; Om, *Oncorhynchus mykiss.*

733 Figure 1

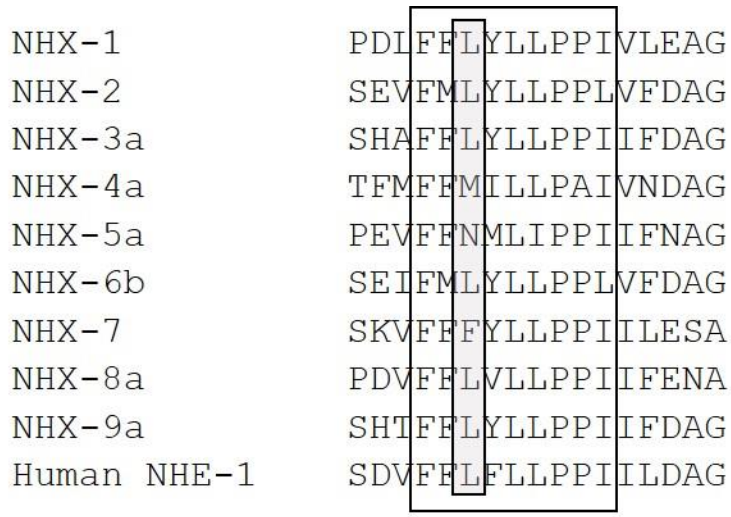

734

735

736 Figure 2:

737

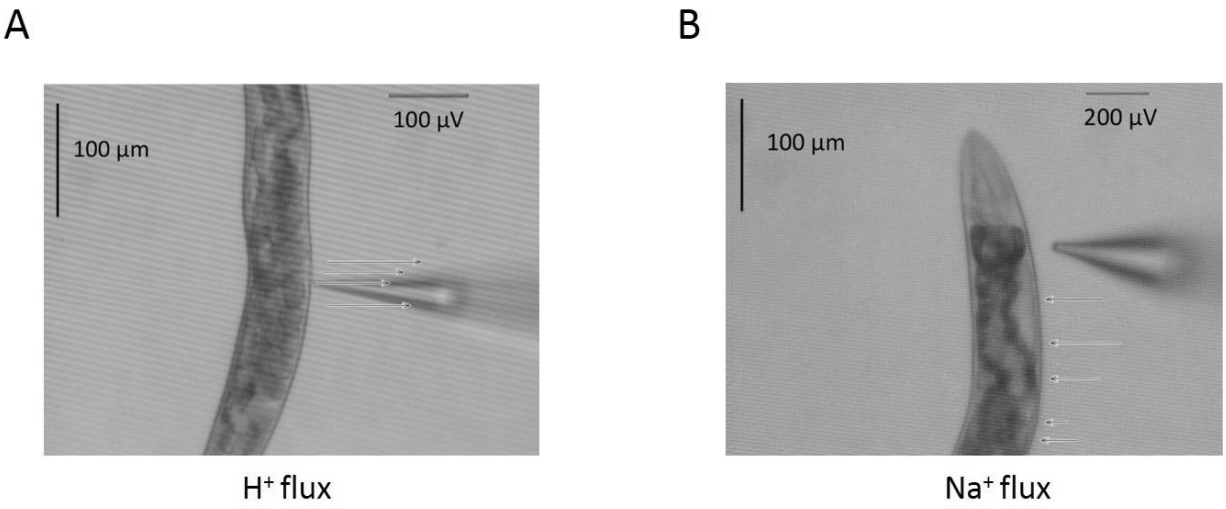

738

739

740

741

742 Figure 3:

743

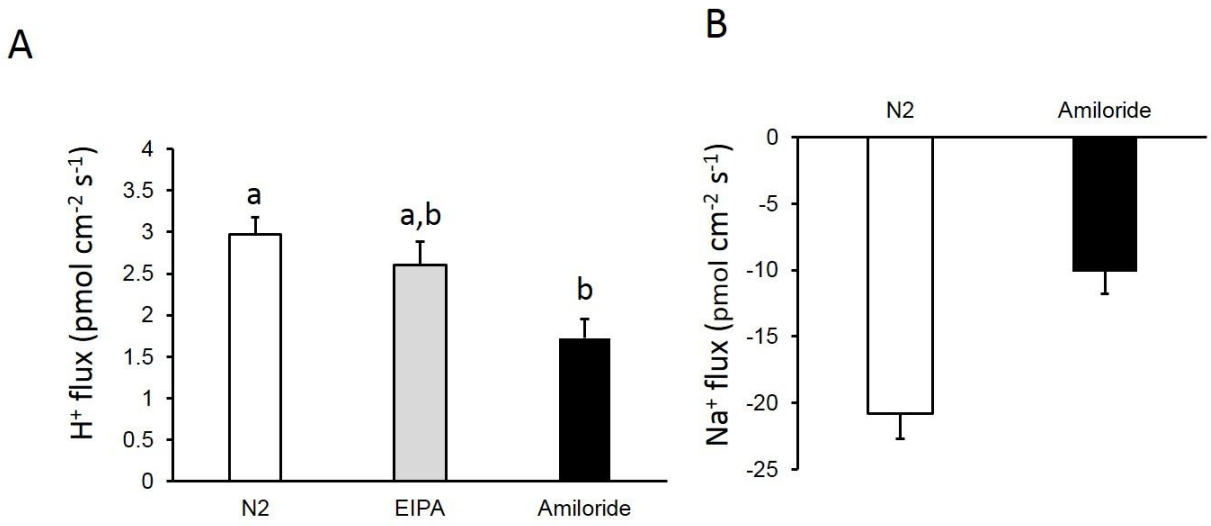

744

745

746

747 Figure 4:

748

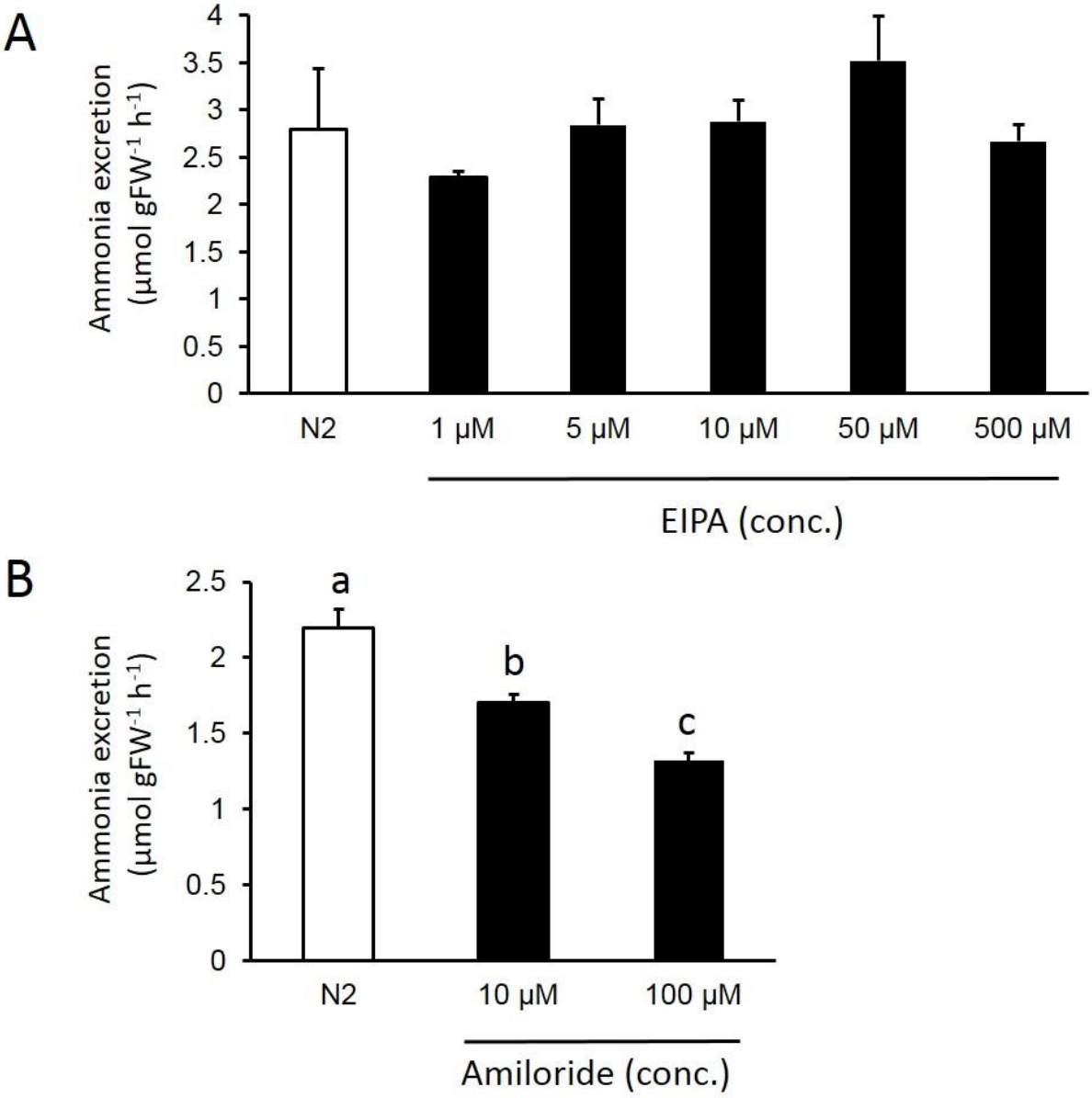

749

750

751

Figure 5:

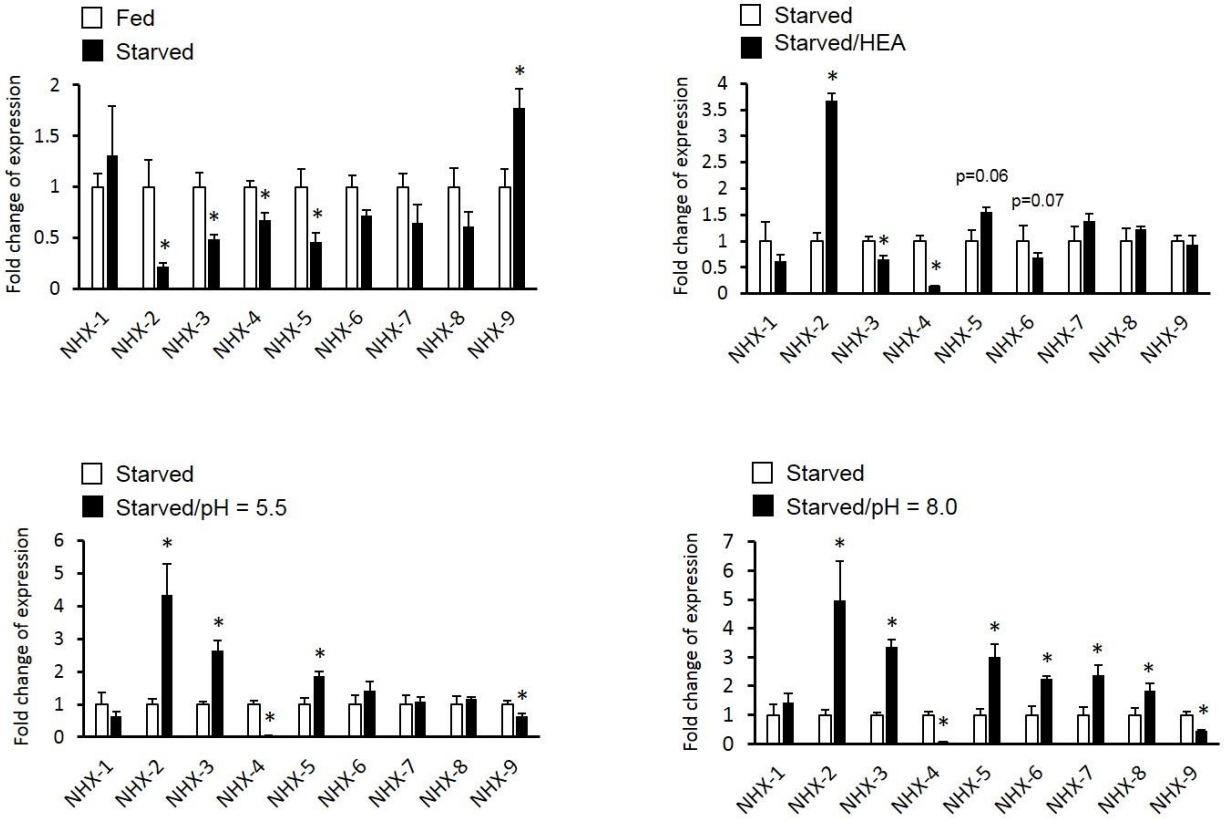
Fed
Starved
Fold change of expression
NHX-1
NHX-2
NHX-3
NHX-4
NHX-5
NHX-6
NHX-7
NHX-8
NHX-9
Starved
Starved/HEA
p=0.06
p=0.07
Starved
Starved/pH = 5.5
Starved
Starved/pH = 8.0

757 Figure 6:

758

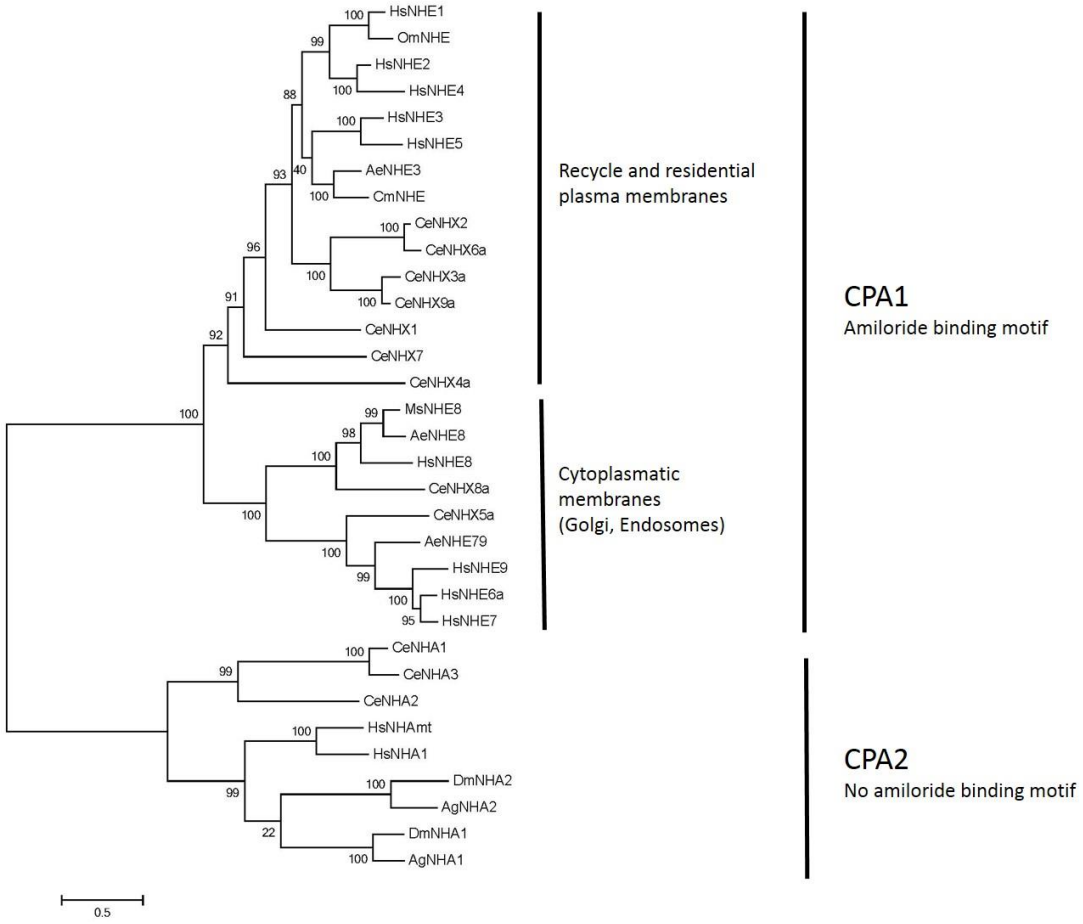

Figure 6

759

760

761

762